

Effect of thermospheric neutral density upon inner trapped-belt proton flux

Thomas L. Wilson,¹ M. A. K. Lodhi,² and Abel B. Diaz²

Abstract

[1] We wish to point out that a secular change in the Earth's atmospheric neutral density alters charged-particle lifetime in the inner trapped radiation belts, in addition to the changes recently reported as produced by greenhouse gases. Heretofore, changes in neutral density have been of interest primarily because of their effect on the orbital drag of satellites. We extend this to include the orbital lifetime of charged particles in the lower radiation belts. It is known that the charged-belt population is coupled to the neutral density of the atmosphere through changes induced by solar activity, an effect produced by multiple scattering off neutral and ionized atoms along with ionization loss in the thermosphere where charged and neutral populations interact. It will be shown here that trapped-belt flux J is bivariant in energy E and thermospheric neutral density ρ , as $J(E,\rho)$. One can conclude that proton lifetimes in these belts are also directly affected by secular changes in the neutral species populating the Earth's thermosphere. This result is a consequence of an intrinsic property of charged-particle flux, that flux is not merely a function of E but is dependent upon density ρ when a background of neutrals is present. **Citation:** Wilson, T. L., M. A. K. Lodhi, and A. Diaz (2007), Effect of

¹ NASA, Johnson Space Center, Code KR, Houston, TX 77058, USA.

² Department of Physics, Texas Tech University, MS 1051, Lubbock, TX 79409, USA.

thermospheric neutral density upon inner trapped-belt proton flux, *Space Weather*, yy, zzzzzz.

1. Introduction

[2] The Earth's thermosphere has been the subject of recent investigations into a possible long-term decrease in its neutral density caused by a change in total mass density at 400 km [*Marcos et al.*, 2005; see also *Emmert et al.*, 2004 and *Keating et al.*, 2000]. Since the thermosphere reacts to solar and geomagnetic conditions in a very complex fashion, a secular decrease in neutral density is not surprising. Energy-momentum deposition into the thermosphere is ultimately traceable to solar activity and takes forms such as Joule heating, particle precipitation, Poynting flux, geomagnetic storm perturbations, and electric fields that drive neutral winds via neutral-ion collisions. The system responds by redistributing mass, energy, and momentum which changes density. The purpose of the present paper is to improve our understanding of the effect of such neutral thermospheric density changes upon charged-particle trapping in the inner radiation belts.

[3] The results of *Marcos et al.* (2005) are based upon orbital perturbation analysis and are particularly interesting because the International Space Station (ISS) and associated Space Shuttle are designed for that altitude. Such studies have depended primarily upon the indirect method of analyzing the orbital decay of satellites to determine the neutral density of the atmosphere, a technique dating back to the beginning of space exploration when the effect of solar activity upon atmospheric density, orbital

drag, and trapped radiation belt populations was discovered by *Jacchia* [1960, 1961, 1963] and *Harris and Priester* [1962a-b, 1963; *Harris and Spencer*, 1968; *Hess*, 1968]. More recently, improved accuracy in estimating density variations has been inferred from accelerometer measurements on satellites such as CHAMP and GRACE [*Bruinsma et al.*, 2006].

[4] The solar radio flux at 10.7 cm, namely $F_{10.7}$, was originally found to be a very good estimate of the effect of solar extreme ultraviolet (EUV) activity upon atmospheric density models even though it was measured at radio and not EUV wavelengths. A picture of the close space environment emerged in which the Earth's atmospheric constituents expand and contract the thermosphere in response to the absorption of varying energy from the Sun during its dynamic cycle of activity. In terms of the Harris and Priester model [1962a], the introduction of solar energy into the atmosphere mentioned earlier takes several forms such as the excitation of atomic and molecular species, photoionization in the EUV, and molecular dissociation. Other forms of heating they considered were charged-particle influx from the inner trapped radiation belts, advection winds, thermal conduction, and chemical reactions. Cooling through radiative transport via atmospheric emission and by alteration of the constituent molecular species were also considered. The latter is the subject of the work in *Marcos et al.* [2005], *Emmert et al.* [2004], and *Keating et al.* [2000]. Collectively, these mechanisms contribute to the thermospheric physical structure (density, temperature, and pressure) as a function of dynamic time-variations which are diurnal (rotation of the Earth), seasonal (orbiting of the Earth about the Sun), and solar-cycle dependent (sunspot activity) – with

isolated perturbations from geomagnetic storms [Bruinsma et al., 2006]. More recent studies of total solar power deposition have shown that solar EUV radiation is the single largest contributor to the upper atmospheric heating budget [Knipp et al., 2005], and $F_{10.7}$ is strongly correlated with EUV [Tobiska, 2001; Lean, 2002]. The exception, however, is the geomagnetic storm [Bruinsma et al., 2006].

[5] The importance of the Harris and Priester model was that it was one of the first to provide a comprehensive analysis of the thermosphere (85-1100 km) as a gas in diffusive equilibrium, for various conditions of solar activity and times of day. Accounting for EUV and $F_{10.7}$ thermal sources, they derived the mean atmospheric mass density ρ from the number densities of constituent species ρ_i (N_2 , O_2 , O, He, and H) from 120 to 2050 km. Their model fundamentally influenced radiation-belt proton research for a number of years. Blanchard and Hess [1964; Hess, 1968] and others [Cornwall et al., 1965; Heckman and Brady, 1966; Dragt, 1971] subsequently used the Harris and Priester model to conclude that the inner-belt proton flux J varied inversely with density ρ , that is $J(\rho) \sim \rho^{-1}$. The present study will show that this conclusion is not entirely correct, and it will give the principal result that the proton flux below 350 MeV is a bivariate function of energy E and mean atmospheric density ρ . It will then relate the trapped-belt lifetime results to the current interest in secular changes in global thermospheric neutral density.

2. Thermospheric Flux Analysis

[6] The method adopted here for analyzing the solar-cycle modulation of the inner trapped-belt proton flux will be a phenomenological one, using a regression algorithm

from nuclear physics [Lodhi and Waak, 1975, 1976] to determine proton flux from the databases available in the original NASA trapped-belt model AP8 [Sawyer and Vette, 1976; Bilitza, 1987], and compare the formulation with the simulation models known as SIREST [Singleterry et al., 2005] and SPENVIS [Heynderickx et al., 2005]. Since AP8 was constructed from satellite data in solar cycle 20, a small one compared to more recent events, its limitations are well known [Watts et al., 1989; Pfitzer, 1990]. Most of those limitations have been overcome with the development of a new computer technique known as NOAAPRO [Huston and Pfitzer, 1998a,b], which has been implemented into SIREST for investigations studying Shuttle and ISS altitudes. A rationale for adopting AP8 was that it is readily available and commonly used [Heynderickx et al., 2004]. Below we demonstrate results that are consistent with the Pfitzer method. Only the omnidirectional fluxes are studied in this analysis, noting that the anisotropic east-west nature of trapped-belt flux such as the South Atlantic Anomaly (SAA) has been discussed by Watts et al. [1989] and Hess [1968] and does not affect our basic conclusion.

[7] The interaction between the inner trapped-belt proton flux and atmospheric neutrals in the Earth's lower thermosphere is depicted in Figure 1 where the iso-contours represent proton flux lines and the north-south asymmetry due to the SAA is evident. Spiraling about magnetic field lines, charged particles propagate north and south until reflected at magnetic-mirror points on each side of the magnetic equator. They continue this back and forth motion in the radiation belts until removed by any of several loss mechanisms, one of which is ionization loss and multiple scattering off of the neutral constituents comprising the atmosphere. As the contours penetrate to lower altitudes

(e.g., at 45° north latitude in Figure 1), the rate of collision and probability of capture or loss in the atmosphere increases. Eventual thermospheric capture means loss from the belt as the charged particle is given up to the atmosphere, serving as a heat source in the thermal balance of the thermosphere. The inner or lower boundary (in altitude above the Earth) of the trapped radiation belt is thus seen to be controlled by atmospheric density. The lifetime and flux J of the resident protons in the inner belt, then, are expected to be inversely proportional to the atmospheric density ρ of the thermosphere [Hess, 1968]. The realization that the atmosphere expands and contracts because of solar activity [Jacchia, 1960, 1961, 1963; Harris and Priester, 1962a-b, 1963] means that there exists a very dynamic coupling between the inner radiation-belt boundary and the thermosphere in Figure 1.

[8] The solar modulation of atmospheric density is taken to be a simple parameterization of the U.S. Air Force Model used by Pfitzer [1990] in his study of ISS dose for altitudes $300 < h < 600$ km for mean atmospheric density ρ

$$\rho = \rho_o \exp \left\{ - (h - 120) / [M(h - 103)^{1/2}] \right\}, \quad (1)$$

where the solar-cycle modulation term M is expressed as

$$M = 0.99 + 0.518 \left\{ (F_{10.7} + F_{bar}) / 110 \right\}^{1/2}, \quad (2)$$

and where ρ_o is assumed to be $\rho_o = 2.7 \times 10^{-11} \text{ g/cm}^3$, h is the altitude in km, $F_{10.7}$ is the instantaneous value of the solar radio flux at 10.7 cm, and F_{bar} is the weighted value of $F_{10.7}$, taken here over the three previous solar rotations. Because the AP8 trapped-belt model is used, solar cycle 20 is necessarily base-lined in the analysis. In the case of that cycle, $F_{10.7}$ is 150 for AP8MAX (the epoch of 1964) and 70 for AP8MIN (the epoch of 1970). As pointed out by Pfitzer, the trapped protons have a very slow response time to dynamic changes in atmospheric density $\rho(t)$. Therefore, the values of $F_{10.7}$ and F_{bar} are assumed identical, whereby $F_{10.7} + F_{bar} = 2 F_{10.7}$ in Equation (2).

[9] Note that the density ρ in Equation (1) is a multi-variant function of h and $F_{10.7}$. Similarly note that the AP8 proton flux J is a multi-variant function of h and energy E . Because altitude h is not an intrinsic property of the Earth's atmosphere, the problem at hand is to generate the multi-dimensional surface of J as a function of E and ρ , or $J(E, \rho)$. In the AP8 model, selecting an altitude h gives the modulated proton flux $J(E)$ as a function of energy E , either at Solar MAX or Solar MIN and nowhere in between. In the model that follows, selecting an instantaneous solar radio flux $F_{10.7}$ emulates the solar cycle and the modulated proton flux $J(E, \rho)$ follows as a bivariate function of energy E and density ρ at *any* time throughout a selected solar cycle.

[10] This bivariate analysis of Equation (1) is illustrated in Figure 2. A "carpet" plot technique was used by *Pfitzer* [1990] as a pragmatic means for dealing with the presence of altitude h in the atmospheric model of Equation (1) when studying dose, and was recently adapted by *Lodhi et al.* [2005a] to show how it could be applied to simulating trapped-belt flux between Solar MAX and Solar MIN. By taking the inverse of Equation

(1) for constant surfaces of $F_{10.7}$ and altitude h respectively, altitude $h = f(\rho)$ and solar radio flux $F_{10.7} = g(\rho)$ as a function of atmospheric density ρ in Equation (1) are obtained from the carpet plot in Figure 2.

[11] The algorithm adopted here is taken from theoretical nuclear physics [Lodhi and Waak, 1975, 1976], using a polynomial regression to determine the functional relationship between trapped-belt fluxes at Solar MIN and Solar MAX. As mentioned, proton lifetime τ is determined by energy losses primarily due to multiple Coulomb scattering and neutral scattering from thermospheric constituents, being a function of epoch time t , proton energy E , and atmospheric density ρ . That is, $\tau = \tau(E, \rho^{-1}, t)$ since the atmosphere dynamically expands and contracts at different times during the solar cycle.

[12] The Galactic Cosmic-Ray (GCR) flux is usually identified as the source of the inner trapped-belt particles, by creating albedo neutrons when colliding with the Earth's atmosphere which then decay into the protons that spiral in the inner belts [Hess, 1968, Ch. 3; see also Battiston (2002)]. The explanation is as follows. At Solar MIN, the GCRs penetrate deeper into the inner solar system than at Solar MAX, and therefore the neutron albedo would seem to be greater for certain energies when solar activity is minimum with the consequence that trapped proton flux is greater at Solar MIN than at Solar MAX. That is, $J_{min}(E) > J_{max}(E)$, using the usual representation of flux J as a mono-variant function of E , or $J(E) \text{ cm}^{-2}\text{s}^{-1}\text{MeV}^{-1}$. Due to the geomagnetic cutoff, only higher energy GCRs can reach the low equatorial latitudes in Figure 1 where albedo

neutron decay produces most of the inner belt protons. Since high-energy GCRs are not modulated appreciably, one might conclude that solar modulation (Solar MIN and MAX) does not play a contributing role in inner-belt proton variations. However, the AP8 model clearly shows such a dependence below 350 MeV. For a given altitude, it produces two such curves, $J_{min}(E)$ for Solar MIN and $J_{max}(E)$ for Solar MAX. The task at hand is to produce a functional relationship between $J_{min}(E)$ and $J_{max}(E)$ from AP8 data.

[13] When utilizing the regression analysis technique, the regression coefficient is kept greater than 90%. A ratio J_{max}/J_{min} is generated for differential proton fluxes as a function of inverse-density ρ^{-1} for energies of concern for ISS between 30 and 300 MeV from AP8 model data at altitudes 300 to 600 km. This ratio is fitted to a polynomial ranging from linear to fifth-order in ρ^{-1} for proton energies of 30, 35, 40, 45, 50, 60, 70, 80, 90, 100, 125, 150, 175, 200, and 300 MeV. Note that this ratio is of non-linear order in ρ^{-1} . One also finds that polynomials of higher-order than second result in a better fit for given energy than the second-order. A common expression for the entire energy range gets worse than that of the second-order, an observation that limits the method to be confined to a second-order expression for the flux ratio as a function of ρ^{-1} for all energies. The regression analysis works well within the energy and altitude range of ISS interest. For other ranges of approximation one has to be careful and repeat the analysis, piecewise fitting the entire dynamical range selected.

[14] Given the premise that $J(\rho) \sim \rho^{-1}$ in the lower thermosphere [Hess, 1968], the regression algorithm technique [§13] is now applied to determine a more accurate functional relationship from AP8. After several trials the best-fitted function thus obtained is given as follows:

$$J_{max}/J_{min} = (a_4 E^4 + a_3 E^3 + a_2 E^2 + a_1 E + a_0) \rho^{-2} + (b_3 E^3 + b_2 E^2 + b_1 E + b_0) \rho^{-1} + (c_2 E^2 + c_1 E + c_0) \quad , \quad (3)$$

for all energies E under consideration. This expression is further approximated by writing the coefficients in exponential form, thus yielding:

$$J_{max}/J_{min} = A e^{\alpha E} \rho^{-2} + B e^{\beta E} \rho^{-1} + C e^{\gamma E} \quad (4)$$

for proton energy ranges from 30 to 300 MeV. Specifically, Equation (4) is

$$J_{max}/J_{min} = -0.0241 e^{0.0007E} \rho^{-2} + 0.1966 e^{-0.0007E} \rho^{-1} + 0.3208 e^{+0.0032E} \quad , \quad (5)$$

with ρ^{-1} in units of $10^{+15} \text{ cm}^3/\text{g}$. This result is illustrated in Figure 3 and Figure 4. To the order of approximation, Equation (3) can be written

$$J(E,\rho) \sim J_o \sum [\sum A_{n+2}(E^{n+2})] \rho^{-n} \quad , \quad (6)$$

giving the bivariate relationship of $J(E,\rho)$ with respect to any chosen reference flux J_o (in this case, J_{min}) on the differential flux surface in Figure 4. The dependence of $J(E,\rho)$ upon background neutrals is particularly helpful in understanding the anomalous cosmic-ray (ACR) flux which is made up of components of the heliospheric neutral atmosphere that can reach the inner solar system and help populate the Earth's radiation belts, a topic that has been addressed elsewhere [Lodhi *et al.*, 2005b].

[15] The result of *Marcos et al.* [2005] that there is a long-term decrease in mean thermospheric neutral density ρ , is seen to affect the proton flux in Equation (6) by virtue of its secular change in the neutral species densities ρ_i that comprise ρ in the Earth's atmosphere. Although the Harris and Priester model did not consider the greenhouse gases CO_2 and CH_4 , the conclusion is the same. As ρ decreases, the penetration depth of the inner trapped-belt protons into the lower thermosphere increases and their lifetime does as well.

3. Conclusions

[16] The proton differential flux in the Earth's inner trapped proton belts has been expressed by a reparameterization of the AP8 model as a bivariate function of energy and density, namely $J(E,\rho) \sim J_o \sum [\sum A_{n+2}(E^{n+2})] \rho^{-n}$. The method provides the potential for evaluating proton intensity as a function of time through the density's dependence on solar $F_{10.7}$. This leads to two principal conclusions: (1) Long-term secular changes in thermospheric density not only affect global temperatures but inner trapped-belt particle life-times as well; (2) The conventional picture that particle flux J is a mono-variant function of energy $J(E)$ is not an accurate one, since an actual characterization comprises a bivariate two-dimensional surface $J(E,\rho)$ that is a function of background neutral density ρ and is correlated with $F_{10.7}$. For the harder portion of general cosmic ray spectra, flux is mono-variant but below ~ 350 MeV it becomes sensitive to the presence of any neutral backgrounds, and like plasmas these are ubiquitous in space. This accounts for what has often been referred to as a time-dependence in J due to solar activity for $E < 350$ MeV, while it is explained here as the presence of a neutral background which in turn is modulated by solar activity. In the technique suggested here, the variation is due to the presence of neutrals ρ and is clearly illustrated in Figure 4.

[17] Acknowledgement. The authors thank an anonymous reviewer for helpful comments during the evaluation of this paper.

References

- Battiston, R. (2002), The Alpha Magnetic Spectrometer, a particle physics experiment in space, *International J. Mod. Phys. A*, *17*, 1589-1601.
- Bilitza, D. (1987), Models of the trapped particle fluxes AE-8 (electrons) and AP8 (protons) in inner and outer radiation belts, Nat. Spa. Sci. Data Center, Goddard Space Flight Center, NSSDC, October.
- Blanchard, R. C., and W. N. Hess (1964), Solar cycle changes in inner-zone protons, *J. Geophys. Res.*, *69*, 3927-3938.
- Bruinsma, S., J. M. Forbes, R. S. Nerem, and X. Zhang (2006), Thermosphere density response to the 20-21 November 2003 solar and geomagnetic storm from CHAMP and GRACE accelerometer data, *J. Geophys. Res.*, *111*, A06303, doi:10.1029/2005JA011284.
- Cornwall, J. M., A. R. Sims, and R. S. White (1965), Atmospheric density experienced by radiation belt protons, *J. Geophys. Res.*, *70*, 3099-3111.
- Dragt, A. J. (1971), Solar cycle modulation of the radiation belt proton flux, *J. Geophys. Res.*, *76*, 2313-2344.
- Emmert, J. T., J. M. Picone, J. L. Lean, and S. H. Knowles (2004), Global change in the thermosphere: Compelling evidence of a secular decrease in density, *J. Geophys. Res.*, *109*, A02301, doi:10.1029/2003JA010176.

- Harris, I., and W. Priester (1962a), Time-dependent structure of the upper atmosphere, *J. Atmos. Sci.*, *19*, 286-301.
- Harris, I., and W. Priester (1962b), Theoretical models for the solar-cycle variation of the upper atmosphere, *J. Geophys. Res.* *67*, 4585-4591.
- Harris, I., and W. Priester (1963), Relation between theoretical and observational models of the upper atmosphere, *J. Geophys. Res.*, *68*, 5891.
- Harris, I., and N. W. Spencer (1968), The Earth's atmosphere, in *Introduction to Space Science*, ed. W. N. Hess and G. D. Mead, Ch. 2, pp. 93-131, Gordon and Breach, New York.
- Heckman, H. H., and V. O. Brady (1966), Effective atmospheric losses for 125-MeV protons in South Atlantic anomaly, *J. Geophys. Res.*, *71*, 2791-2798.
- Hess, W. N. (1968), *The Radiation Belt and Magnetosphere*, Ch. 1, p. 11, and Ch. 4, p. 139, Blaisdell, London.
- Heynderickx, D., *et al.*, 2004. SPace ENVironment Information System (SPENVIS), European Space Agency (ESA), <http://www.spennis.oma.be/spennis/>.
- Huston, S. L., and K. A. Pfizter (1998a), A new model for the low altitude trapped proton environment, *IEEE Trans. On Nuclear Science*, *45*, no. 6, 2972-2978.
- Huston, S.L., and K. A. Pfizter (1998b), Space environment effects: Low-altitude trapped radiation models, Marshall Space Flight Center, NASA/CR-1998-208593, 63 pp., available at <http://see.msfc.nasa.gov/ire/irepub.html>.
- Jacchia, L.G. (1960), A variable atmospheric-density model from satellite accelerations, *J. Geophys. Res.*, *65*, 2775-2782.

- Jacchia, L.G. (1961), A working model for the upper atmosphere, *Nature*, *192*, 1147-1148.
- Jacchia, L.G. (1963), Variations in the Earth's upper atmosphere as revealed by satellite drag, *Rev. Mod. Phys.*, *35*, 973-991.
- Keating, G. M., R. H. Tolson, and M. S. Bradford (2000), Evidence of long term global decline in the Earth's thermospheric densities apparently related to anthropogenic effects, *Geophys. Res. Lett.*, *27*, 1523-1526.
- Knipp, D. J., W. K. Tobiska, and B. A. Emery (2005), Direct and indirect thermospheric heating sources for solar cycles 21-23, *Solar Phys.*, *224*, 495-505.
- Lean, J. L. (2002), Comment on "Validating the solar EUV proxy, $F_{10.7}$ " by W. K. Tobiska, *J. Geophys. Res.*, *107*, No. A2, 10.1029/2001JA000137.
- Lodhi, M. A. K., A. B. Diaz, and T. L. Wilson (2005a), Simplified solar modulation model of inner trapped belt proton flux as a function of atmospheric density, *Rad. Meas.*, *39*, 391-399.
- Lodhi, M. A. K., A. B. Diaz, and T. L. Wilson (2005b), Influence of interstellar neutrals as an atmosphere on charged-particle flux in the heliosphere, *Proc. Joint Meeting of the Nuclear Physics Div. of the Amer. Phys. Soc. and the Japanese Phys. Soc.*, Maui, Hawaii, September 18-22, CF.00012.
- Lodhi, M. A. K., and B. T. Waak (1975), Solution of bound state problems in nuclear shell models with momentum-dependent potentials, *Comm. Phys. Comm.*, *10*, 182-193.

- Lodhi, M. A. K., and B. T. Waak (1976), A momentum-dependent potential approximated by the Morse function for studying nuclear systematics, *Ann. Phys.*, *101*, 1-21.
- Marcos, F. A., J. O. Wise, M. J. Kendra, N. J. Grossbard, and B. R. Bowman (2005), Detection of a long-term decrease in thermospheric neutral density, *Geophys. Res. Lett.*, *32*, L04103, doi:10.1029/2004GL021269.
- Pfitzer, K. A. (1990), Radiation dose to man and hardware as a function of atmospheric density in the 28.5 degree Space Station orbit, McDonnell Douglas Space Systems Co., Advanced Technology Center, Huntington Beach, CA 92647, MDSSC Rep. No. H5387 Rev. A.
- Ray, E. C. (1960), On the theory of protons trapped in the Earth's magnetic field, *J. Geophys. Res.*, *65*, 1125-1134.
- Sawyer, D. M., and J. I. Vette (1976), AP8 trapped proton environment for solar maximum and solar minimum, Nat. Spa. Sci. Data Center, Goddard Space Flight Center, NSSDC/WDC-A-R&S 76-06.
- Singleterry, R., *et al.* (2004), Space Ionizing Radiation Environments and Shielding Tools (SIREST), NASA Langley, <http://sirest.larc.nasa.gov/>.
- Tobiska, W. K. (2001), Validating the solar EUV proxy, $F_{10.7}$, *J. Geophys. Res.*, *106*, 29,969-29,978.
- Watts, J. W., T. A. Parnell, and H. H. Heckman (1989), Approximate angular distribution and spectra for geomagnetically trapped protons in low-Earth orbit. In: *High-Energy Radiation Background in Space*, Rester, A.C., Jr., and Trombka, J.I.

(Eds.), *AIP Conf. Proc.*, 186, New York, 75-85.

Figure 1 Caption

Interaction of the inner trapped-belt protons with the atmospheric neutrals in the Earth's lower thermosphere. Taken from 1958 detector data at various altitudes showing contours of relative count rates, at west longitudes of 60° - 20° in the neighborhood of the South Atlantic Anomaly. Adapted from *Hess* [1968].

Figure 2 Caption

A carpet plot, illustrating the bivariate relationship $\rho = \rho(h, F_{10.7})$ between atmospheric density ρ , altitude h , and solar modulation parameter $F_{10.7}$ in Equation (1).

Figure 3 Caption

Comparison of the algorithm in Equation (5) with AP8 mono-variant flux $J(E)$ at solar maximum during Cycle 20 for various Shuttle and ISS altitudes h (350, 400, 450, 500, 550, and 600 km) assuming $F_{10.7} = F_{bar} = 110$. This is the conventional representation of trapped-belt flux $J(E)$ as a function of energy E for various altitudes h in Equation (1). The altitude h , however, is not an intrinsic property of the atmospheric background.

Figure 4 Caption

Proton differential flux $J(E,\rho)$ versus energy E and density ρ at the altitudes in Figure 3, having eliminated h using Figure 2. The effect of the background neutral density ρ is to spread the flux J over a bivariant surface $J(E,\rho)$, demonstrating the three-dimensional nature of flux when neutrals are present.

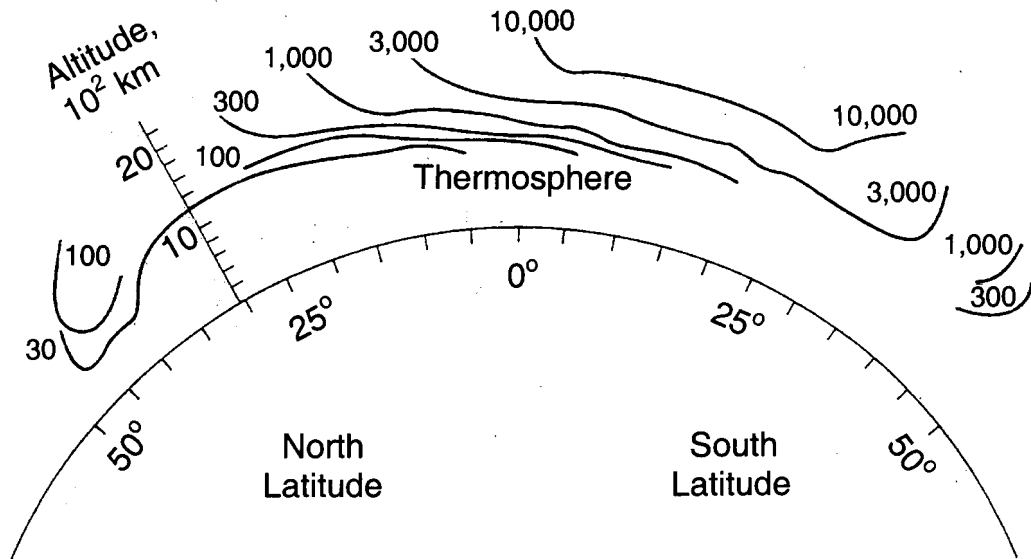


Figure 1. Interaction of the inner trapped-belt protons with the atmospheric neutrals in the Earth's lower thermosphere. Taken from 1958 detector data at various altitudes showing contours of relative count rates, at west longitudes of 60° - 20° in the neighborhood of the South Atlantic Anomaly. Adapted from *Hess* [1968].

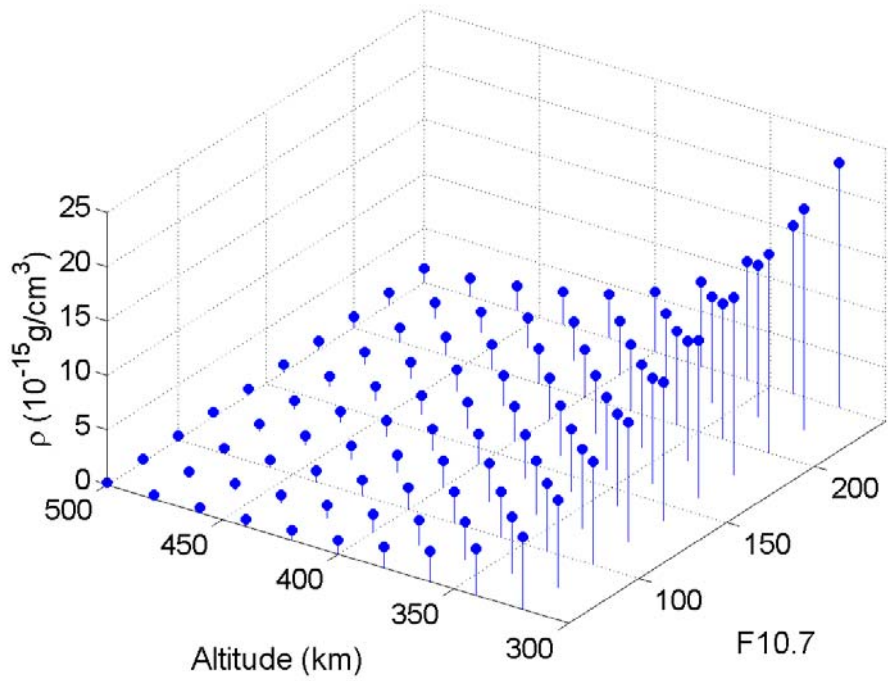


Figure 2. A carpet plot, illustrating the bivariate relationship $\rho = \rho(h, F_{10.7})$ between atmospheric density ρ , altitude h , and solar modulation parameter $F_{10.7}$ in Equation (1).

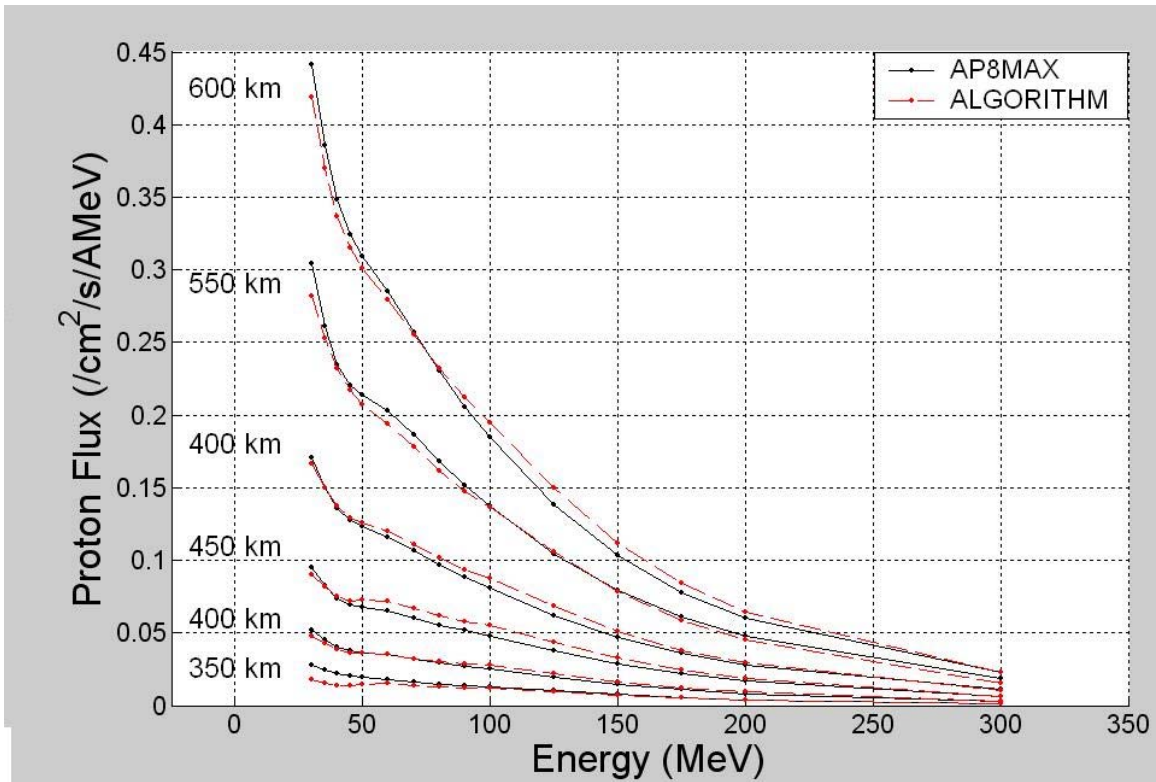


Figure 3. Comparison of the algorithm in Equation (5) with AP8 mono-variant flux $J(E)$ at solar maximum during Cycle 20 for various Shuttle and ISS altitudes h (350, 400, 450, 500, 550, and 600 km) assuming $F_{10.7} = F_{bar} = 110$. This is the conventional representation of trapped-belt flux $J(E)$ as a function of energy E for various altitudes h in Equation (1). The altitude h , however, is not an intrinsic property of the atmospheric background.

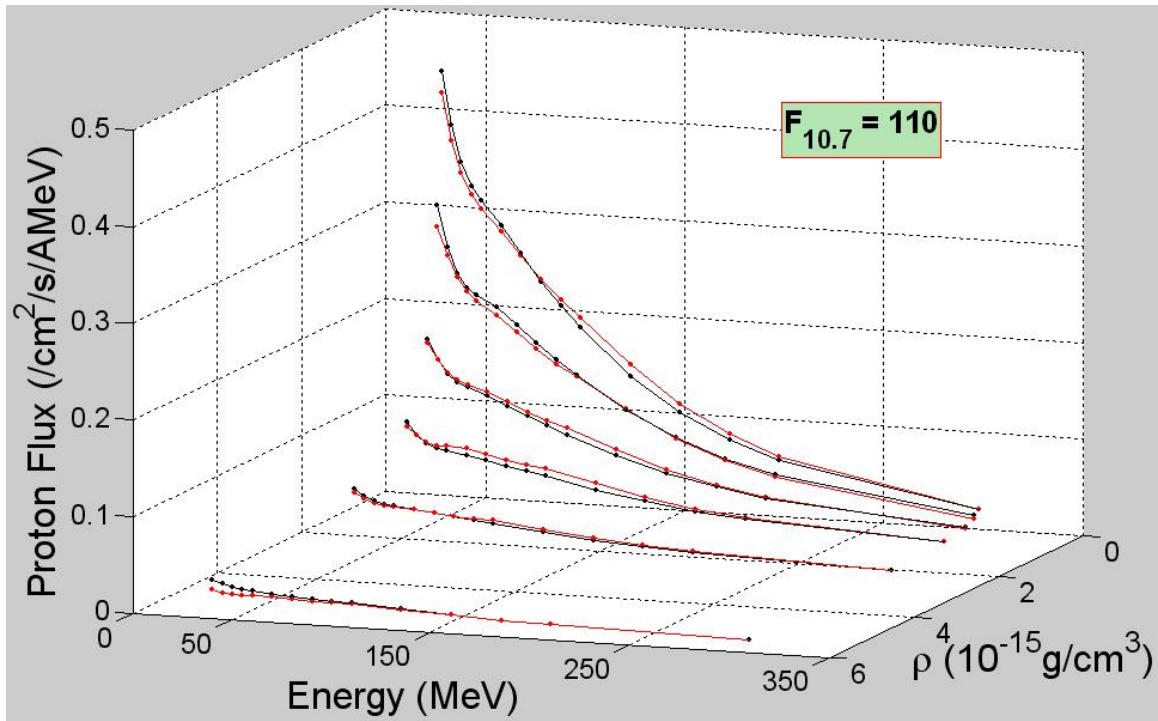


Figure 4. Proton differential flux $J(E,\rho)$ versus energy E and density ρ at the altitudes in Figure 3, having eliminated h using Figure 2. The effect of the background neutral density ρ is to spread the flux J over a bivariant surface $J(E,\rho)$, demonstrating the three-dimensional nature of flux when neutrals are present.